A Benchmark Pairs Details

In Appendix A.1 we discuss the details of high-dimensional benchmark pairs. Appendix A.2 is devoted to Celeba 64×64 images benchmark pairs.

A.1 High-dimensional Benchmark Pairs

The benchmark creation example is given in Figure 1. In each dimension we fix random Gaussian mixtures $\mathbb{P}, \mathbb{Q}_1, \mathbb{Q}_2$ (in the code we hard-code the random seeds) and use them to create a benchmark.

To generate a random mixture of M Gaussian measures in dimension D, we use the following procedure. Let $\delta, \sigma > 0$ (we use $\delta = 1, \sigma = \frac{2}{5}$) and consider the M-dimensional grid

$$G = \{-\frac{\delta \cdot M}{2} + i \cdot \delta \text{ for } i = 1, 2, \dots, M\}^D \subset \mathbb{R}^D.$$

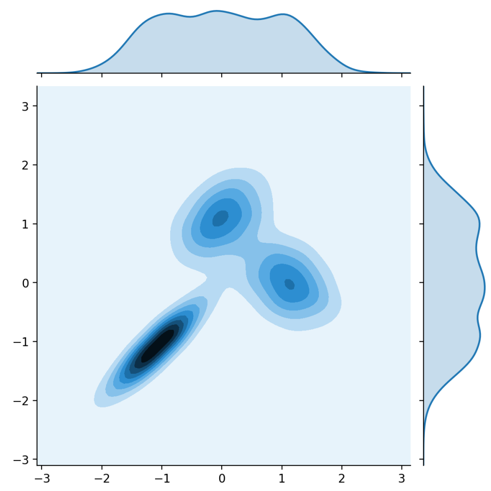
(a) A random mixture of 3 Gaussians.

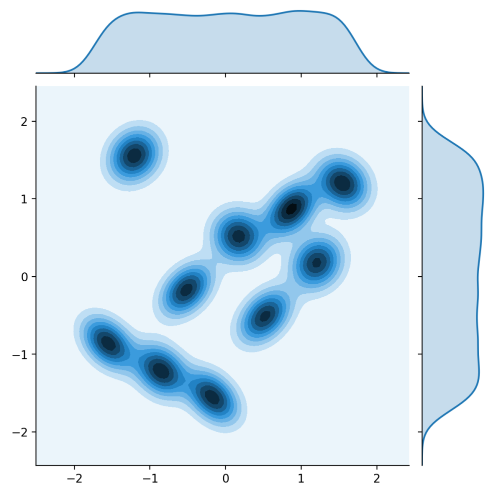
(b) A random mixture of 10 Gaussians.

Figure 6: Randomly generated Gaussian mixtures. Projection on to first two dimensions.

We pick M random points $\mu'_1, \dots \mu'_M \in G$ such that no pair of points has any shared coordinate. We initialize random $A'_1, \dots, A'_M \in \mathbb{R}^{D \times D}$, where each row of each matrix is randomly sampled from $D-1$ dimensional sphere in $\mathbb{R}^D$. Let $\Sigma'_m = \sigma^2 \cdot (A'_m) \cdot (A'_m)^\top$ for $m = 1, 2, \dots, M$ and note that $[\Sigma'_m]_{dd} = \sigma^2$ for $d = 1, 2, \dots, D$. Next, we consider the Gaussian mixture $\frac{1}{M}\sum_{m=1}^{M} \mathcal{N}(\mu'_m, \Sigma'_m)$. Finally, we normalize the mixture to have axis-wise variance equal to 1, i.e. we consider the final mixture $\frac{1}{M}\sum_{m=1}^{M} \mathcal{N}(\mu_m, \Sigma_m)$, where $\mu_m = a\mu'_m$ and $\Sigma_m = a^2\Sigma_m$. The value $a \in \mathbb{R}_+$ is given by

$$a^{-1} = \sqrt{\frac{\sum_{m=1}^{M} \|\mu'_m\|^2}{M \cdot D} + \sigma^2}.$$

Gaussian mixtures created by the procedure have D same nice marginals, see Figure 6.

A.2 CelebA 64×64 Images Benchmark Pairs

We fit 3 generative models on CelebA64 aligned faces dataset with a 128-dimensional latent Gaussian measure to sample from their distribution, using WGAN-QC [19] with a ResNet generator network. For trials $k = 1, 2$, we keep generator checkpoints after $1000, 5000, 10000$ iterations to produce measures $\mathbb{Q}^k_{\text{Early}}, \mathbb{Q}^k_{\text{Mid}}, \mathbb{Q}^k_{\text{Late}}$ respectively. In the last trial $k = 3$, we keep only the final generator network checkpoint after 50000 iterations which produces measure $\mathbb{P}^3_{\text{Final}}$. To make each of measures absolutely continuous, we add white Normal noise (axis-wise $\sigma = 0.01$) to the generators' output.

We use the generated measures to construct images benchmark pairs according to the pipeline described in §4.1. We visualize the pipeline in Figure 2.

B Experimental Details

In Appendix B.1, we discuss the neural network architectures we used in experiments. All the other training hyperparameters are given in Appendix B.2.

B.1 Neural Network Architectures

In Table 4 below, we list all the neural network architectures we use in continuous OT solvers. In every experiment we pre-train networks to satisfy $\nabla\psi_\theta(x) = x - \nabla f_\theta(x) \approx x$ and $H_\omega(y) \approx y$ at the start of the optimization. We empirically noted that such a strategy leads to more stable optimization.

Solver	High-dimensional benchmark	CelebA benchmark	CelebA image generation
⌊LS⌉	$\psi_\theta, \phi_\omega : \mathbb{R}^D \to \mathbb{R}$ - DenseICNN (U)	N/A	
⌊MM-B⌉	$\psi_\theta : \mathbb{R}^D \to \mathbb{R}$ - DenseICNN (U)	$f_\theta : \mathbb{R}^D \to \mathbb{R}$ - ResNet	
⌊QC⌉	$\psi_\theta : \mathbb{R}^D \to \mathbb{R}$ - DenseICNN (U)	$f_\theta : \mathbb{R}^D \to \mathbb{R}$ - ResNet	
⌊MM⌉	$\psi_\theta : \mathbb{R}^D \to \mathbb{R}$ - DenseICNN (U) $H_\omega : \mathbb{R}^D \to \mathbb{R}^D$ - ∇ of DenseICNN (U)	$f_\theta : \mathbb{R}^D \to \mathbb{R}$ - ResNet $H_\omega : \mathbb{R}^D \to \mathbb{R}^D$- UNet	
⌊MM:R⌉	$T_\theta : \mathbb{R}^D \to \mathbb{R}^D$ - ∇ of DenseICNN (U) $\phi_\omega : \mathbb{R}^D \to \mathbb{R}$ - DenseICNN (U)	$T_\theta : \mathbb{R}^D \to \mathbb{R}^D$- UNet $g_\omega : \mathbb{R}^D \to \mathbb{R}$ - ResNet	
⌊MMv1⌉	$\psi_\theta : \mathbb{R}^D \to \mathbb{R}$ - DenseICNN	N/A	
⌊MMv2⌉ ⌊W2⌉	$\psi_\theta : \mathbb{R}^D \to \mathbb{R}$ - DenseICNN $H_\omega : \mathbb{R}^D \to \mathbb{R}^D$ - ∇ of DenseICNN	$\psi_\theta : \mathbb{R}^D \to \mathbb{R}$ - ConvICNN64 $H_\omega : \mathbb{R}^D \to \mathbb{R}^D$ - ∇ of ConvICNN64	
⌊MMv2:R⌉ ⌊W2:R⌉	$T_\theta : \mathbb{R}^D \to \mathbb{R}^D$ - ∇ of DenseICNN $\phi_\omega : \mathbb{R}^D \to \mathbb{R}$ - DenseICNN	$T_\theta : \mathbb{R}^D \to \mathbb{R}^D$ - ∇ of ConvICNN64 $\phi_\omega : \mathbb{R}^D \to \mathbb{R}$ - ConvICNN64	

Table 4: Network architectures we use to parametrize potential f (or ψ) and map H in tested solvers. In the reversed solvers we parametrize second potential g (or ϕ) and forward transport map T by neural networks.

In the **high-dimensional benchmark**, we use DenseICNN architecture from [16, §B.2]. It is a fully-connected neural net with additional input-quadratic skip-connections. This architecture can be made input-convex by limiting certain weights to be non-negative. We impose such as a restriction only for ⌊MMv1⌉,⌊MMv2⌉,⌊W2⌉ solvers which require networks to be input-convex. In other cases, the network has no restrictions on weights and we denote the architecture by DenseICNN (U). In experiments, we use the implementation of DenseICNN from the official repository of ⌊W2⌉ solver

`https://github.com/iamalexkorotin/Wasserstein2GenerativeNetworks`

More precisely, in the experiments with probability measures on $\mathbb{R}^D$, we use

$$\text{DenseICNN}[1; \max(2D, 64), \max(2D, 64), \max(D, 32)].$$

Here 1 is the rank of the input-quadratic skip connections and the other values define sizes of fully-connected layers the sequential part of the network. The notation follows [16, §B.2].

We emphasize that DenseICNN architecture ψ_θ has diffirentiable CELU [4] activation functions. Thus, $\nabla\psi_\theta$ is well-defined. In particular, artificial $\beta \cdot \|x\|^2/2$ for $\beta = 10^{-4}$ is added to the output of the last layer of the ICNN. This makes ψ_θ to be β-strongly convex. As the consequence, $\nabla\psi_\theta$ is a bijective function with Lipschitz constant lower bounded by β, see the discussion in [16, §B.1].

In the **experiments with CelebA images**, for parametrizing the potential $f = f_\theta : \mathbb{R}^D \to \mathbb{R}$ in ⌊MM⌉, ⌊QC⌉, ⌊MM-B⌉, we use ResNet architecture from the official WGAN-QC [19] repository:

`https://github.com/harryliew/WGAN-QC`

To parametrize the map $H = H_\omega : \mathbb{R}^D \to \mathbb{R}^D$ in ⌊MM⌉ solver, we use UNet architecture from

`https://github.com/milesial/Pytorch-UNet`

In ⌊MMv2⌉, ⌊W2⌉ solvers we parametrize $\psi = \psi_\theta$ and $H = H_\omega = \nabla\phi_\omega$, where both ψ_θ, ϕ_ω have ConvICNN64 architecture, see Figure 7. We artificially add $\beta \cdot \|x\|^2/2$ (for $\beta = 10^{-4}$) to the output of the output of the ConvICNN64 to make its gradient bijective.

In the architecture, *PosConv2D* layers are usual 2D convolutional layers with all weights (except biases) restricted to be non-negative. *Conv2D-CQ* (convex quadratic) are fully convolutional blocks

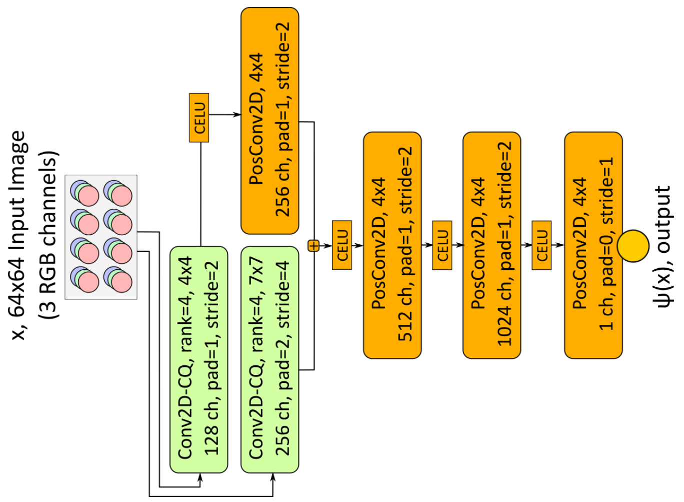

Figure 7: Convolutional ICNN architecture we use for processing 64×64 RGB images.

which output a tensor whose elements are input-quadratic functions of the input tensor. In Figure 8, we present the architecture of Conv2D-CQ block. Here, *GroupChannelSumPool* operation corresponds to splitting the tensor per channel dimension into n_{out} sequential sub-tensors (each of r channels) and collapsing each sub-tensor into one 1-channel tensor by summing r channel maps. The layer can be viewed as the convolutional analog of *ConvexQuadratic* dense layer proposed by [16, §B.2].

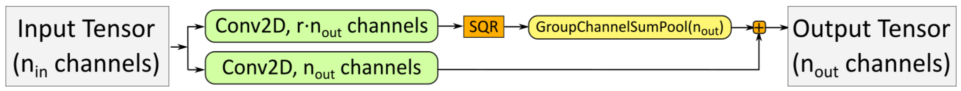
Input Tensor
(n_{in} channels)
Conv2D, $r \cdot n_{out}$ channels
SQR
GroupChannelSumPool(n_{out})
Conv2D, n_{out} channels
Output Tensor
(n_{out} channels)

Figure 8: 2D convolutional convex quadratic block.

In the **CelebA image generation experiments**, we also use ResNet architecture for the generator network g. The implementation is taken from WGAN-QC repository mentioned above.

B.2 Hyperparameters and Implementation Details

The evaluation of all the considered continuous solvers for evaluation is not trivial for two reasons. First, not all the solvers have available user-friendly *Python* implementations. Next, some solvers are not used outside the GAN setting. Thus, for considering them in the benchmark, proper extraction of the $\mathbb{W}_2$ solver (discriminator part) from the GAN is needed.

We implement most of the solvers from scratch. In all the cases, we use Adam optimizer [15] with default hyperparameters (exept the learning rate). For solvers $\lfloor$QC$\rceil$ by [19] and $\lfloor$W2$\rceil$ by [16] we use the code provided by the authors in the official papers' GitHub repositories.

B.2.1 High-dimensional Benchmark Pairs

We report the hyper parameters we use in high-dimensional benchmark in Table 5. *Total iterations* column corresponds to optimizing the potential f_θ (or ψ_θ) to *maximize* the dual form (8). In maximin solvers, there is also an inner cycle which corresponds to solving the inner *minimization* problem in (8). The hyperparameters are chosen empirically to best suit the considered evaluation setting.

For $\lfloor$QC$\rceil$ solver large batch sizes are computationally infeasible since it requires solving a linear program at each optimization step [19, §3.1]. Thus, we use batch size 64 as in the original paper. $\lfloor$W2$\rceil$ solver is used with the same hyperparameters in training/evaluation of the benchmarks.

B.2.2 CelebA 64×64 Images Benchmark Pairs

For the images benchmark, we list the hyperparameters in Table 6.

Solver	Batch Size	Total Iterations	LR	Note
⌊LS⌉	1024	100000	10^{-3}	Quadratic regularization with $\epsilon = 3 \cdot 10^{-2}$, see [36, Eq. (7)]
⌊MM-B⌉	1024	100000	10^{-3}	None
⌊QC⌉	64	100000	10^{-3}	OT regularization with $K = 1, \gamma = 0.1$, see [19, Eq. (10)]
⌊MMv1⌉	1024	20000	10^{-3}	1000 gradient iterations ($lr = 0.3$) to compute argmin in (8), see [39, §6]. Early stop when gradient norm $< 10^{-3}$.
⌊MM⌉,⌊MMv2⌉	1024	50000	10^{-3}	15 inner cycle iterations to update H_ω, ($K = 15$ in the notation of [26, Algorithm 1])
⌊W2⌉	1024	250000	10^{-3}	Cycle-consistency regularization, $\lambda = D$, see [16, Algorithm 1]

Table 5: Hyperparameters of solvers we use in high-dimensional benchmark. Reversed are not presdented in this table: they use the same hyperparameters as their original versions.

Solver	Batch Size	Total Iterations	LR	Note
⌊MM-B⌉	64	20000	$3 \cdot 10^{-4}$	None
⌊QC⌉	64	20000	$3 \cdot 10^{-4}$	OT regularization with $K = 1, \gamma = 0.1$, see [19, Eq. (10)]
⌊MM⌉	64	50000	$3 \cdot 10^{-4}$	5 inner cycle iterations to update H_ω, ($K = 5$ in the notation of [26, Algorithm 1])
⌊W2⌉	64	50000	$3 \cdot 10^{-4}$	Cycle-consistency regularization, $\lambda = 10^4$, see [16, Algorithm 1]

Table 6: Hyperparameters of solvers we use in CelebA images benchmark.

B.2.3 CelebA 64×64 Images Generation Experiment

To train a generative model, we use GAN-style training: generator network G_α updates are alternating with OT solver's updates (discriminator's update). The learning rate for the generator network is $3 \cdot 10^{-4}$ and the total number of generator iterations is 50000.

In ⌊QC⌉ solver we use the code by the authors: there is one gradient update of OT solver per generator update. In all the rest methods, we alternate 1 generator update with 10 updates of OT solver (*iterations* in notation of Table 6). All the rest hyperparameters match the previous experiment.

The generator's gradient w.r.t. parameters α on a mini-batch $z_1, \dots, z_N \sim \mathbb{S}$ is given by

$$\partial \mathbb{W}_2^2(\mathbb{P}_\alpha, \mathbb{Q}) / \partial\alpha = \int_z \mathbf{J}_\alpha G_\alpha(z)^T \nabla f^*\big(G_\alpha(z)\big) d\mathbb{S}(z) \approx \frac{1}{N}\sum_{n=1}^{N} \mathbf{J}_\alpha G_\alpha(z_n)^T \nabla f_\theta\big(G_\alpha(z_n)\big) \qquad (10)$$

where $\mathbb{S}$ is the latent space measure and f_θ is the current potential (discriminator) of OT solver. Note that in ⌊MM:R⌉ potential f is not computed but the forward OT map T_θ is parametrized instead. In this case, we estimate the gradient (10) on a mini-batch by $\frac{1}{N}\sum_{n=1}^{N} \mathbf{J}_\alpha G_\alpha(z_n)^T(\text{id}_{\mathbb{R}^D} - T_\theta)$.